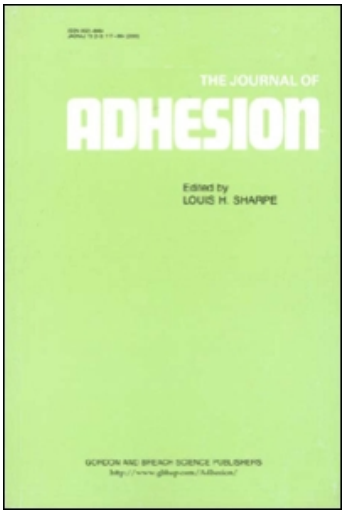

The Journal of Adhesion
Publication details, including instructions for authors and subscription information:
http://www.informaworld.com/smpp/title~content=t713453635

The Effects of Cure Temperature and Time on the Bulk Tensile Properties of a Structural Adhesive

Erol Sancaktar[a]; Hooshang Jozavi[a]; Robert M. Klein[a]
[a] Department of Mechanical and Industrial Engineering, C/arkson College of Technology, Potsdam, N. Y., U.S.A.

To cite this Article Sancaktar, Erol , Jozavi, Hooshang and Klein, Robert M.(1983) 'The Effects of Cure Temperature and Time on the Bulk Tensile Properties of a Structural Adhesive', The Journal of Adhesion, 15: 3, 241 — 264
To link to this Article: DOI: 10.1080/00218468308073230
URL: http://dx.doi.org/10.1080/00218468308073230

J. Adhesion, 1983, Vol. 15, pp. 241–264
0021–8464/83/1504–0241 $18.50/0

Printed in Great Britain

The Effects of Cure Temperature and Time on the Bulk Tensile Properties of a Structural Adhesive

EROL SANCAKTAR, HOOSHANG JOZAVI and ROBERT M. KLEIN

Department of Mechanical and Industrial Engineering, Clarkson College of Technology, Potsdam, N.Y. 13676, U.S.A.

(*Received July 12, 1982; in final form December 3, 1982*)

The effects of cure time and temperature as well as cool-down rate on the adhesive tensile properties, yield stress (σ_y) and elastic modulus (E), were determined experimentally. Commercially available, solid film Metlbond 1113 (with carrier cloth) and 1113–2 (without carrier cloth) adhesives were used as model adhesives. The experimentally determined tensile properties were used to calculate theoretically the critical stain energy release rate (G_{IC}) based on the radius of the crack tip deformation zone reported by Bascom. The calculated G_{IC} values were then compared with the measured values which are available in the literature. The comparison revealed good agreement between the calculated and measured G_{IC} values.

INTRODUCTION

The tensile strength and rigidity of adhesives are known to depend on the cure temperature, time and cool-down conditions.[1,2] This suggests that the adhesive fracture stress is also dependent on the cure conditions. Adhesively bonded joint failures are usually results of catastrophic crack propagations originating from inherent flaws (trapped air bubbles) and impurities.[3,4] Hence, complete characterization of adhesives requires an investigation of the fracture stresses as a function of different cure and service conditions.

A measure of the fracture stress that occurs in the vicinity of a crack tip is the strain energy release rate. An investigation of the strain energy release rate as a function of different cure conditions will, therefore, reveal information on the variation of the fracture stress with respect to the same cure conditions.

The effects of cool-down rates on the critical strain energy release rate have been investigated by O'Connor.[5] He reports that a short cool-down period results in lower values of G_{IC} compared to those obtained with longer cool-down periods.

The dominant mode of failure for bonded joints (particulary for the single lap joint geometry) is the opening mode (Mode-I).[6] For this reason, investigation of the effects of cure conditions on the Mode-I strain energy release rate (G_I) will provide information which can be related to the majority of in-service bonding conditions.

This paper presents results on the effects of cure temperature, time and cool-down rates on the critical strain energy release rate (G_{IC}), elastic tensile modulus (E), and yield strength (σ_y), of a structural epoxy adhesive, with and without carrier cloth. The effects of cure temperature and time on the bulk tensile properties are investigated experimentally, first. These experimental results also provide information on the effects of carrier cloth and cure pressure. The optimization behavior of adhesive strength (σ_y) and rigidity (E) with respect to the cure conditions for both types of adhesives (with and without the carrier cloth) are obtained subsequently.

Before proceeding further, it will be appropriate to define what is meant by the "optimization behavior." Since there are two parameters involved (namely cure temperature and cure time) strength (or rigidity) *vs.* cure temperature curves are plotted for different cure time conditions. An envelope curve is then fitted through the maxima of these curves. This envelope curve is called the "optimization curve." Any maximum on this envelope curve represents the optimum point with respect to cure temperature and time.

It is possible to calculate theoretical G_{IC} values based on proposed relations by using the above mentioned experimental results. Thus, calculation of the optimization behavior for the theoretical G_{IC} values with respect to the cure conditions is also possible.

Inherent flaws usually cause the bondline to fail in a brittle manner.[3,4] The presence of a carrier cloth also affects the fracture pattern. A previous investigation on the Metlbond adhesive[5] reported that slow crack propagation (a result of ductile fracture) occurred along a plane

of fiber while fast crack propagation (a result of brittle fracture) was confined to planes without fiber.

As fracture processes affect the bonded adhesive behavior dominantly, it becomes necessary to determine accurate relations for the fracture stresses as a function of various design and service parameters. If the adhesive behaves in a brittle manner (in the bonded form), then the use of a LEFM (Linear Elastic Fracture Mechanics) approach can be considered appropriate for characterizing the fracture stresses.

The model adhesives chosen for the project are Metlbond 1113 and 1113-2 which are commercially available from Narmco Materials, Inc. (Costa Mesa, California) in $\sim$0.01 in. and $\sim$0.005 in. thick rolls, respectively. As described by the manufacturer, Metlbond 1113 is a 100% solid, modified epoxy film with a synthetic carrier cloth. Metlbond 1113-2 is identical to 1113 without the carrier cloth. Both types of adhesives are chosen in order to obtain information on the effects of the carrier cloth at different cure conditions.

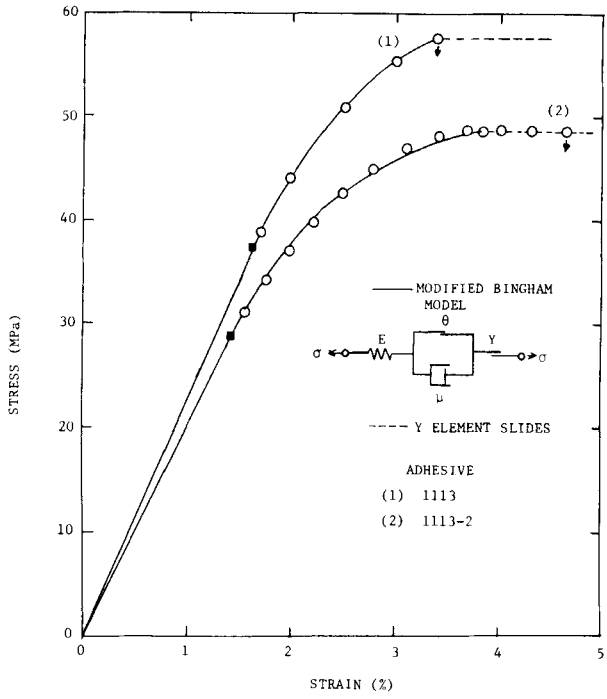

FIGURE 1 Tensile stress–strain behavior of the Metlbond adhesive with 2 in/min (5.08 cm/min) Head Rate (Ref. 9).

Metlbond 1113 and 1113-2 were used as model adhesives during a number of previous investigations.[3,4,5,7,8,9] These investigations included tensile[8,9] and bonded fracture testing[5] of the same adhesives. Even though the G_{IC} and tensile properties *vs.* cure temperature and time data are not available from these works, the availability of some tensile and bonded fracture data and the successful use of the adhesive for testing purposes were the main reasons for choosing the Metlbond as the model adhesive for the present investigation.

Brinson *et al.*[8,9] previously determined that the mechanical behavior of Metlbond 1113 and 1113-2 adhesives (Figure 1) is affected by the rate of straining. They showed that the constant strain rate stress–strain behavior of the adhesives approaches a perfectly elastic–plastic behavior as the magnitude of the strain rate is increased.

For structural adhesives, an elastic–plastic mechanical behavior assumption has been used widely by investigators such as Bascom[6] and Hart-Smith.[10] Bascom[6] used a crack tip plane–strain assumption to relate the adhesive yield stress, tensile modulus and the radius of the crack tip deformation zone to the critical strain energy release rate. This way, he was able to calculate a theoretical value for the radius of the crack tip deformation zone by using his experimentally measured values of G_{IC}, σ_y, and E.[11–14] Apparently, if information on the radius of the crack tip deformation zone (r_y) is available, then one can calculate the G_{IC} values directly from the tensile properties. Bascom[6,15] reports the magnitude of r_y as $\sim 8 \times 10^{-3}$ in. for a CTBN-epoxy (Carboxy-Terminated Butadiene-Acrylonitrile).

Experimentally measured G_{IC} values for Metlbond 1113-2 adhesive are available in the literature.[5] Information in regard to the effects of cure conditions on the G_{IC}, however, is yet to be obtained.

Adhesive manufacturers generally do not supply detailed information on the variation of the tensile properties with cure times and temperatures. When data are available they are usually limited to the (lap) joint strength of adhesives. For example, the product information brochure[16] for the UHU-PLUS (UHU Linger and Fischer, 758 Bühl Baden, W. Germany) adhesive reports that the thermosetting resin/hardener system reaches maximum lap joint strength values at the following cure time–temperature schedules: 180 minutes at 104°F, 45 minutes at 185°F, 10 minutes at 212°F, and 5 minutes at 302°F–356°F. The brochure also states that high joint strength is obtained at high cure temperatures. Reportedly, the lap joint strength (4258 psi) obtained with cure at 356°F for 5 minutes is twice that obtained with cure at 68°F for 20 hours.

Objectives

The objectives of this investigation were:

1) to optimize the adhesive strength *vs.* cure temperature and time behavior,

2) to optimize the adhesive rigidity *vs.* cure temperature and time behavior,

3) to determine the effect of the cool-down conditions on the above mentioned strength-cure and rigidity-cure optimization behaviors,

4) to determine the effect of the carrier cloth on the strength-cure and the rigidity-cure optimization behaviors,

5) to calculate the G_{IC} values based on a proposed relation and thus to determine the critical strain energy release rate–cure optimization behavior.

EXPERIMENTAL PROCEDURE

Manufacturer's product information for the model adhesives Metlbond 1113 and 1113-2[17] states that typical mechanical properties can be obtained with the following cure conditions:

	Low Temperature Cure	Standard Cure	Fast Cure
Temperature (°F)	200	260	290
Time (Minutes)	120	30	20
Pressure (psi)	15–50	15–50	15–50

Previous investigations[3,8] have shown that the adhesive tensile properties are much easier to measure in the bulk form as compared to the bonded form. This is due to the fact that the bulk specimens are not affected by the interfacial and geometrical factors which may govern the bonded behavior.[4,7] The same argument is also valid for the measurement of G_{IC} with the use of DCB or TDCB specimens. Furthermore, bulk measurements accurately describe the bonded adhesive behavior with cohesive failure, when geometrical factors affecting the stress state are accounted for.

Specimen preparation

All tests are performed by using dog-bone type tensile specimens in the bulk form (Figure 2). The specimen preparation process can be summarized as follows:

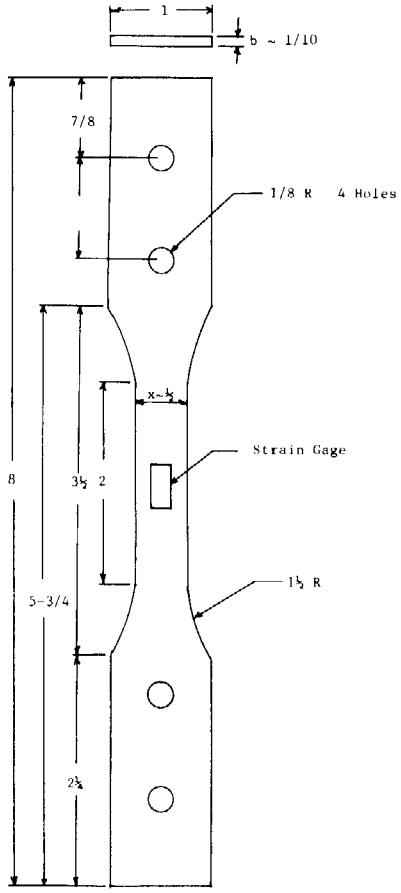

FIGURE 2 Dog-bone bulk tensile specimen (all dimensions are in inches).

1) The roll of adhesive is removed from cold storage (~30°F) and allowed to reach ambient temperature.

2) Eighteen 1–1/2 × 9 in. pieces of the adhesive are cut to make one

Metlbond 1113-2 specimen (eleven plies are needed for Metlbond 1113 specimens).

3) Aluminum plates which have 1–1/2 × 9 × 0.1 in. grooves machined in them are used to cure the adhesive specimens. Teflon is sprayed on these plates to ensure the release of the cured specimens. The eighteen pieces of the adhesive are then placed one at a time into the plate and smoothed with a gloved hand in order to get rid of as many air bubbles as possible.

4) The plates and the adhesive are then placed in the center of the oven which is at ambient temperature and atmospheric pressure. The oven (manufactured by Applied Testing Systems, Saxonburg, PA) is a forced convection type and is equipped with a temperature controller. The oven controller is then set to the desired cure temperature. A thermocouple wrapped in adhesive, to simulate the adhesive temperature, is connected to the controller for monitoring the temperature. When the desired cure temperature is attained, timing is begun for the cure time chosen. The cure time is the amount of time the specimen is in the oven and the cure temperature is the temperature in the oven. Cure schedules with cure time settings of 20 minutes, 120 minutes, 1000 minutes, 5000 minutes, and 10,000 minutes, corresponding to each cure temperature setting of 115°F, 140°F, 170°F, 200°F, 230°F, 260°F and 290°F are used. For each individual cure condition two cool-down rates are used. These are a) fast cool-down, which is simulated by taking the specimen out of the oven and allowing it to reach ambient temperature, and b) slow cool-down, which is simulated by turning the oven off, leaving its door closed and allowing it to reach the ambient temperature (Figure 3).

5) The cured adhesive is then stored in a low humidity ($\sim 0\%$ relative humidity) and room temperature environment. This is done by storing the cured adhesive with a silica gel desiccant in a tightly sealed container.

6) To facilitate the machining of the specimens, the cured adhesive is taped to a metal template with two-sided tape. A jigsaw is used to remove most of the excess adhesive along the template border. The final shaping is done using a router, where the template slides along a guide pin to ensure a uniform specimen shape. A drill press with a 1/4 in. bit is then used to drill the mounting holes in the specimen. After the holes are drilled, the specimen is removed from the template and smoothed with a sanding block.

7) In order to be able to monitor the strains and to calculate the elastic modulus, electrical resistance strain gages are mounted on the

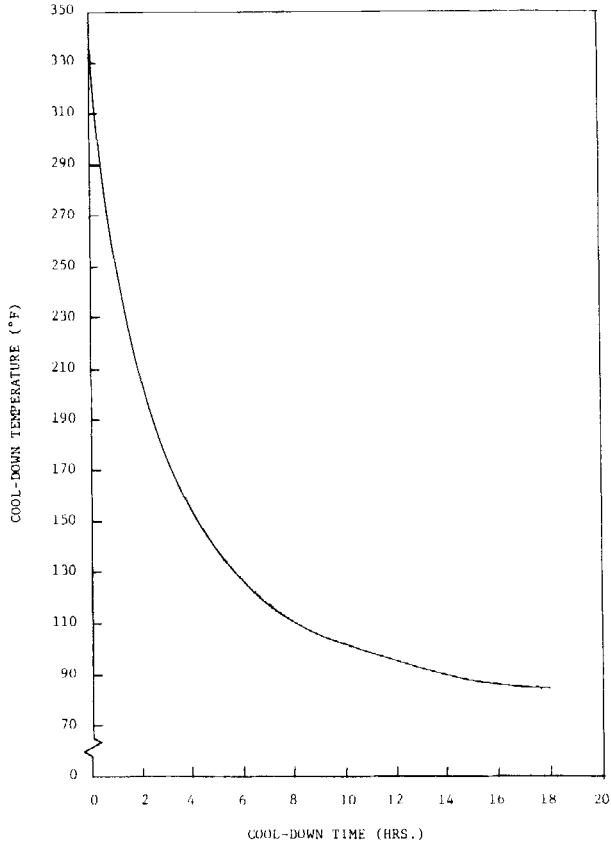

FIGURE 3 Temperature decrease *vs.* time for the slow cool-down condition.

specimens according to the gage manufacturer's directions (Figure 2). The strain gages and the strain gage epoxy are manufactured by the Bean Company.

Test procedure

The first step of the test procedure was to measure the dimensions of x and b (Figure 2) accurately with a vernier caliper. Accuracy of measurement was important because stress as well as the elastic modulus were functions of the cross-sectional area.

All tests were conducted on a Tinius–Olsen universal testing machine

using a constant head rate of 2 in./min. Such a fast head rate was used to minimize the viscoelastic effects. The strip chart on the testing machine was used to record the load *vs.* time. The strain gage signal was amplified through a Vishay bridge amplifier and recorded on a strip chart recorder. All specimens were tested in an environment of approximately 70°F and 65% relative humidity which was maintained with the use of an air conditioning system.

An additional procedure was applied to determine whether there was a density change during the cure process. This was done by carefully weighing a piece of uncured adhesive on a Mettler balance and comparing to the weight of the same piece after cure.

RESULTS AND DISCUSSION

The effects of cure conditions on the tensile strength of Metlbond 1113-2 and 1113 are shown in Figures 4 and 5. A cure temperature *vs.* tensile strength curve is shown for each cure time. The typical "bell-shaped" temperature–strength curves exhibit the increasing–decreasing behavior of the tensile strength with respect to the cure temperature and reveal the existence of the maxima in such behavior. This behavior is in agreement with the results of Chmura and McAbee.[1] These figures also show the optimization curve for the adhesive strength, with respect to the cure temperature and time. The optimization curves are obtained by connecting the maximum points on each "bell-shaped" curve. Therefore, they are based on the cure time durations of 10, 20, 120, 1000, 5000 minutes (and 10,000 minutes for Metlbond 1113) and the fast cool-down condition. The optimization curves exhibit a decrease in tensile strength with increasing cure temperatures and decreasing cure times. The authors attribute this behavior to the increase in randomness of the adhesive crosslink network resulting in lower values of tensile strength. Apparently high temperature short time conditions which were applied in this investigation are far from approximating steady conditions which are better represented by the low temperature long time conditions which were used. Degradation of the latent hardener and the polymer structure itself at high temperatures is also believed to result in lower values of tensile strength. The authors also believe that the magnitudes of the thermal residual stresses which are intensified due to the presence of the carrier cloth are increased at high temperature short time cure conditions, resulting in lower values of tensile strength. These residual stresses also play an important role in

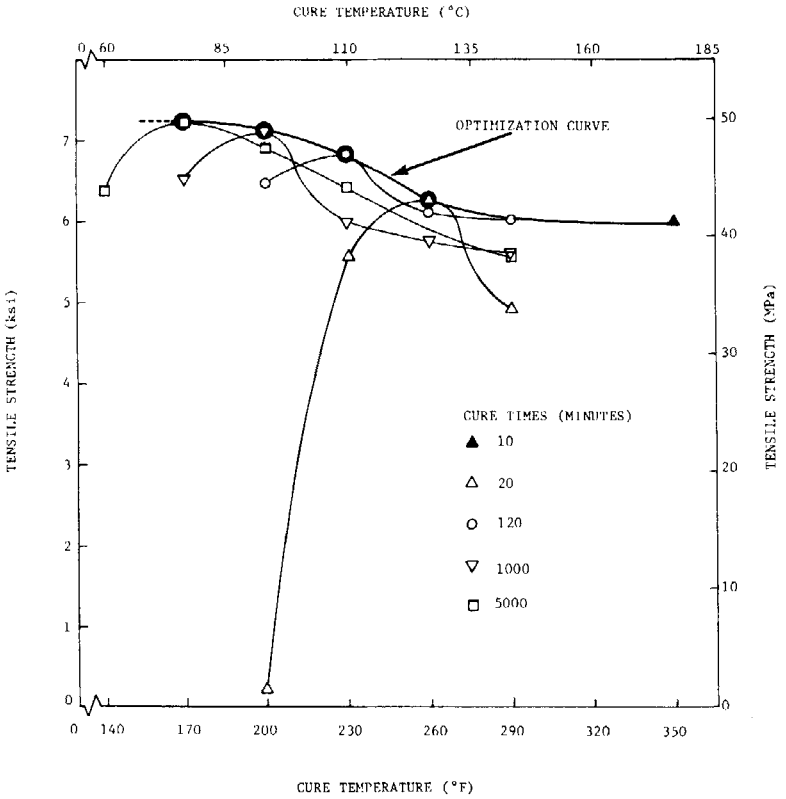

FIGURE 4 Metlbond 1113-2 strength-cure optimization curve for the fast cool-down condition.

the reduction of strength for Metlbond 1113-2, as a relatively large amount of bulk adhesive material (in comparison to Metlbond 1113 with carrier cloth) is being cured.

Figures 6 and 7 show the optimization curves for the elastic moduli with respect to the cure temperature and time for Metlbond 1113-2 and 1113. The optimization curves for the elastic moduli are obtained in the same fashion as that for the tensile strength. Comparisons of Figures 4, 5, 6 and 7 show that the optimization behavior of the elastic moduli is similar to that of the ultimate strengths.

The effects of the cool-down conditions on the tensile strength–cure optimization behavior of Metlbond 1113-2 and 1113 are shown in Figures 8 and 9. Apparently, the slow cool-down condition yields a greater tensile strength in comparison to the fast cool-down condition.

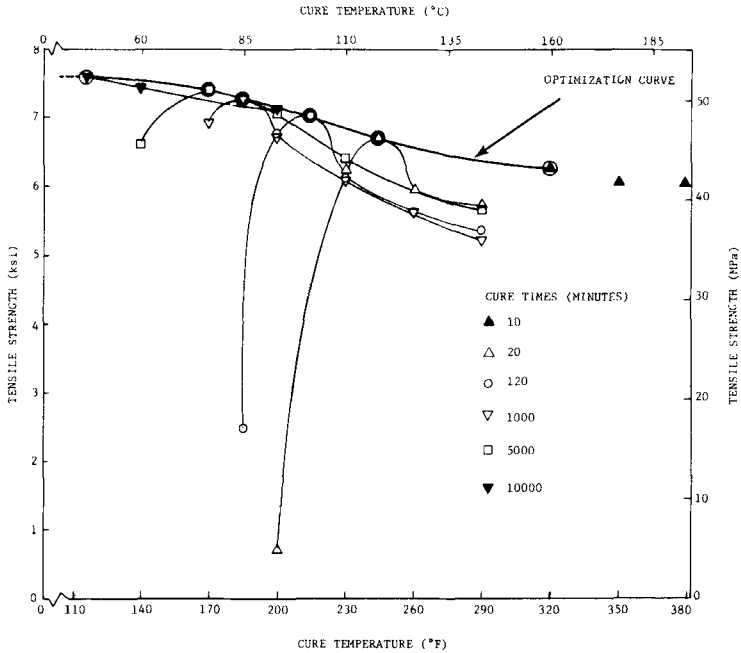

FIGURE 5 Metlbond 1113 strength-cure optimization curve for the fast cool-down condition.

The thermal residual stresses that develop during the initial cure process are relieved during the slow cool-down post-cure period, resulting in a more stable and favorable molecular network structure. Figures 8 and 9 also show that the difference in the tensile strengths, obtained with the fast and slow cool-down conditions, is greater at high cure temperature and short cure times than at low cure temperatures and long cure times. Apparently, the thermal residual stresses that develop during the initial cure process are lower to start with at low temperature and long time cure conditions. In other words, the effects of low temperature–long time cure and slow cool-down are similar.

Thermal stress formation is a function of the thermal gradients present in the bulk adhesive. As high-temperature, short-time cure schedules represent highly unsteady conditions, larger thermal gradients are produced. This situation becomes especially pronounced when a relatively large volume of material is used (Metlbond 1113-2). Therefore, steady (slow) cool-down condition results in relatively higher increases in strength when applied to highly unsteady (high temperature–short

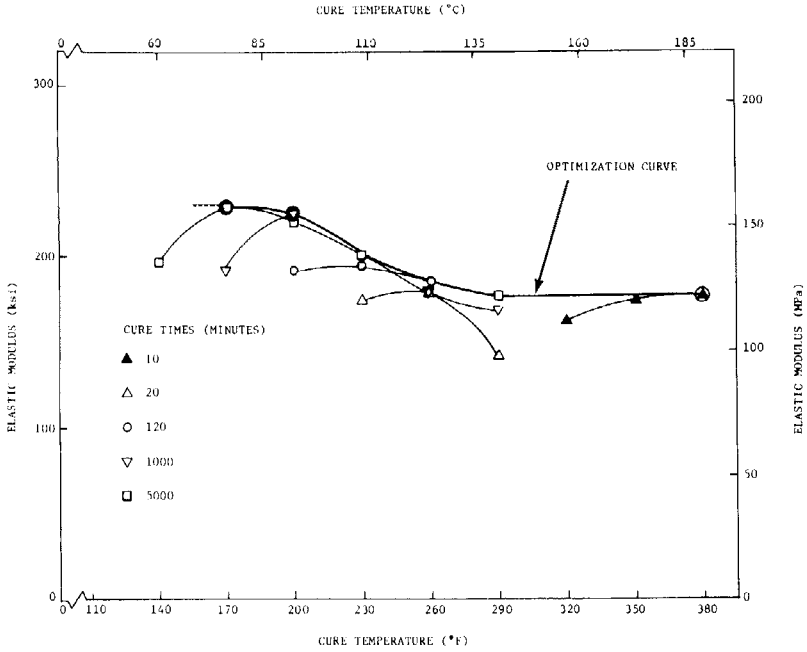

FIGURE 6 Metlbond 1113-2 rigidity-cure optimization curve for the fast cool-down condition.

time) initial cure cycles. The following interpretations may be offered for this effect: (i) the adhesive continues to be cured during the slow cool-down period thus relieving the residual stresses by providing uniform cure, (ii) the thermal residual stresses which may be produced in the already cured adhesive are minimized with the use of slow cool-down which minimizes thermal gradients, (iii) a combination of the two effects mentioned above is present.

A comparison of Figures 8 and 9 reveals the effects of carrier cloth on adhesive tensile strength with the fast and slow cool-down conditions. For the slow cool-down condition the carrier cloth does not show any significant effect on tensile strength. This may be attributed to the effect of the slow cool-down condition in the elimination of thermal residual stresses. For the fast cool-down condition the carrier cloth again does not have any effect on the tensile strength up to (about) 230°F cure temperature. This behavior is similar to the above mentioned behavior with slow cool-down as low temperature–long time conditions are similar to slow cool-down conditions. Past 230°F cure temperature

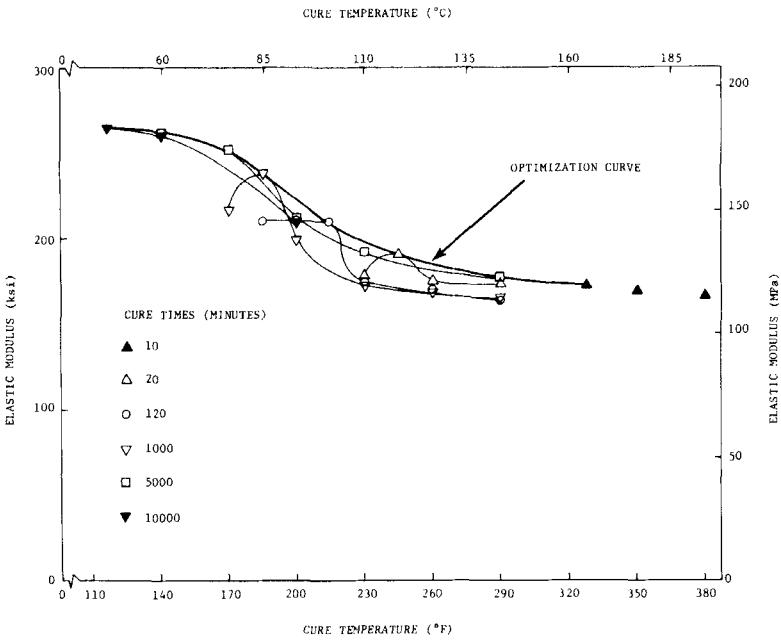

FIGURE 7 Metlbond 1113 rigidity-cure optimization curve for the fast cool-down condition.

(with fast cool-down) the carrier cloth yields higher tensile strength. This behavior is in agreement with the results of Brinson.[8,9]

Comparison of Figure 1 with Figures 8 and 9 reveals the effect of cure pressure on adhesive strength. Brinson's specimens were casted by employing a higher cure pressure as the manufacturer's standard cure procedure was applied,[8,9,16] (see Experimental Procedure Section). Apparently, increasing pressure causes an increase in tensile strength for both Metlbond 1113 and 1113-2. The effect of pressure is greater on Metlbond 1113 than on Metlbond 1113-2.

Figure 10 illustrates the effect of cool-down rate on an individual "bell-shaped" cure temperature *vs.* strength curve. A parallel shift is observed, covering the whole temperature range, except for the lowest temperature value (200°F) where a complete cure is not obtained with the fast cool-down condition. When a slow cool-down condition is used, however, a drastic increase in tensile strength is observed as a result of complete cure with extended heating.

The effect of the cool-down conditions on the rigidity cure optimiza-

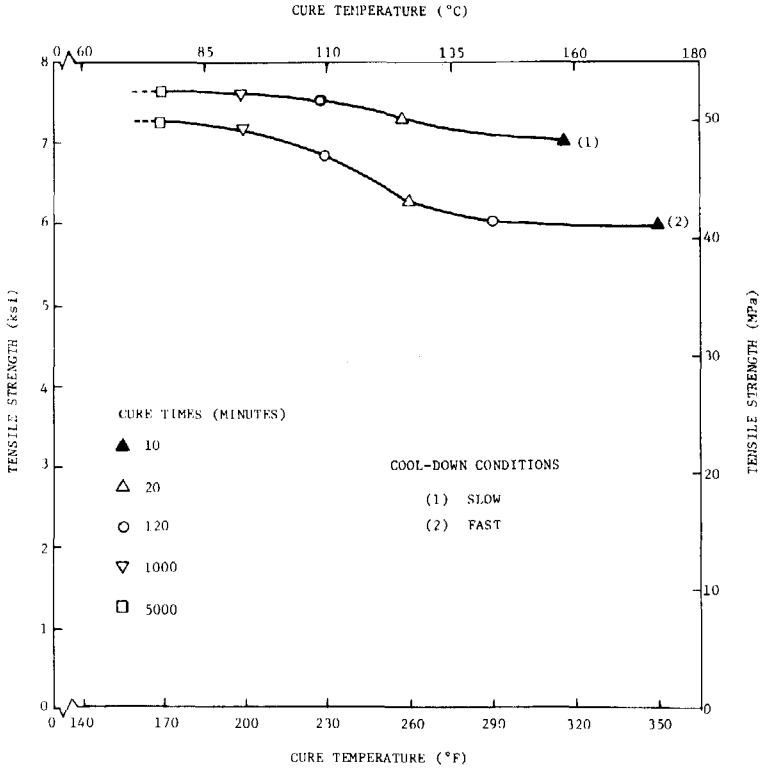

FIGURE 8 Comparison of Metlbond 1113-2 strength-cure optimization curves for the slow and fast cool-down conditions.

tion behavior of Metlbond 1113 is shown in Figure 11. Apparently, the slow cool-down condition yields higher rigidities in comparison to the fast cool-down condition. The rigidity optimization curve obtained with the fast cool-down condition approaches the one obtained with slow cool-down, at low temperature long time cure conditions. This behavior is similar to the one observed in the strength optimization curves obtained with fast and slow cool-down conditions (Figure 9).

Experimental results did not reveal any appreciable effect of the cool-down conditions on the rigidity cure optimization behavior of Metlbond 1113-2. The authors attribute this result to the general increase in ductility of Metlbond 1113-2, when slow cool-down conditions are used. Even though the stress values increase with the slow cool-down

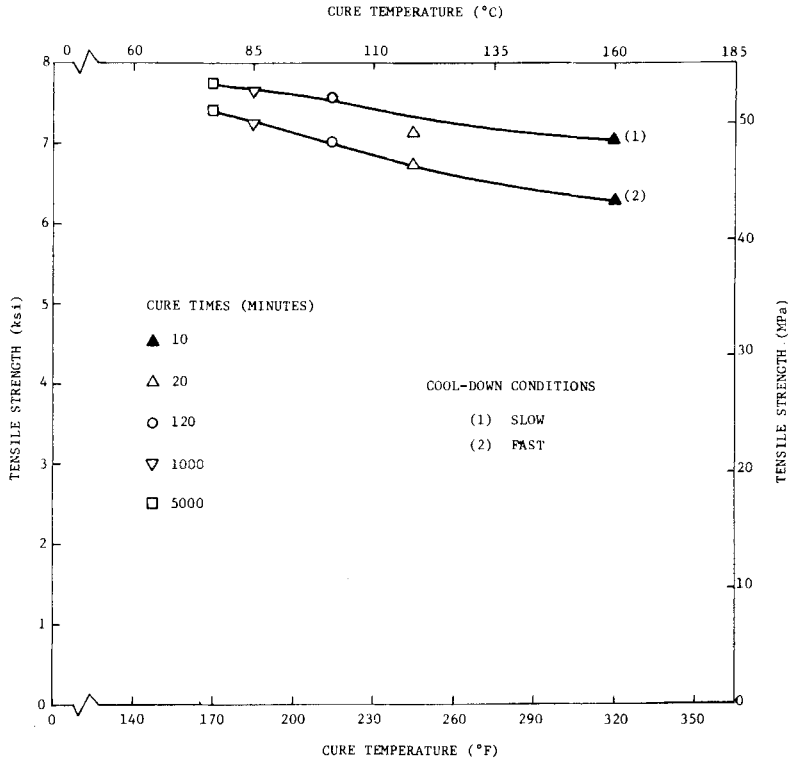

FIGURE 9 Comparison of Metlbond 1113 strength-cure optimization curves for slow and fast cool-down conditions.

condition (as indicated by the increase in tensile strength), the strain values also increase to result in unaffected rigidity values.

Experimental data revealed that, in general, higher cure temperatures result in increased ductility and plastic flow. It was also observed that incomplete cure which occurs at low temperature–short time cure conditions results in low strength brittle material behavior.

As mentioned earlier, the effect of cure temperature on the weight loss of the adhesive was also measured during this investigation. Experimental measurements revealed that an increase in cure temperature increases the amount of weight loss. This increase was determined to be as high as 95%. On the other hand, the overall percentage of the weight loss in comparison to the original weight of the bulk adhesive (prior to cure) was found to be negligible (.287%).

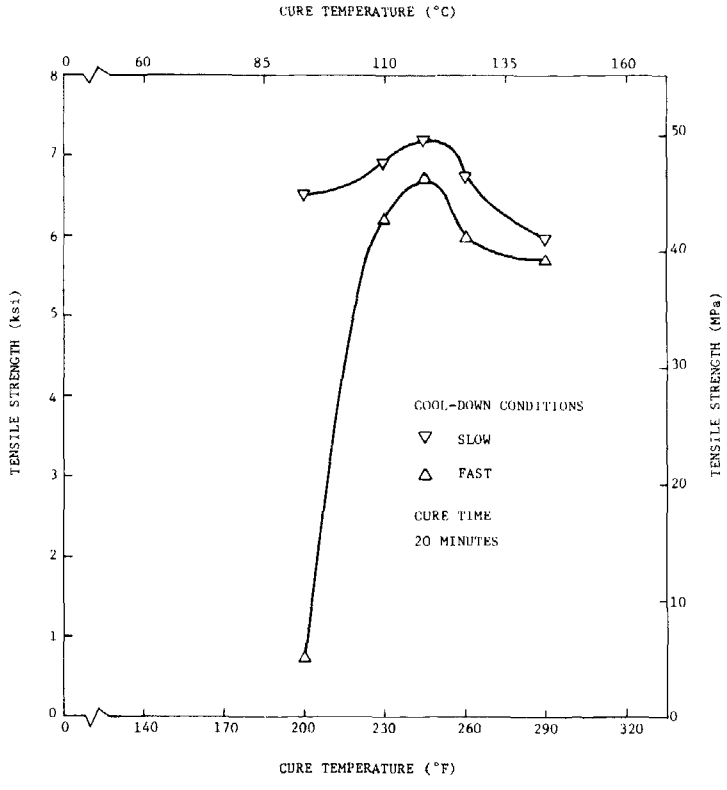

FIGURE 10 The effect of cool-down condition on the tensile strength of Metlbond 1113.

Theoretical calculation of the strain energy release rate

The energy required to propagate a crack with the application of a stress is called the fracture energy. The stress intensity factor (K) is used as a measure of the stress in the vicinity of a crack tip. The stress intensity factor for an isotropic material can be expressed as[18]

$$K = (GE')^{1/2} \tag{1}$$

where G is the strain energy release rate and

$$E' = E/(1 - \nu^2) \tag{2}$$

for the plane–strain condition (ν is the Poisson's ratio). Equation (1)

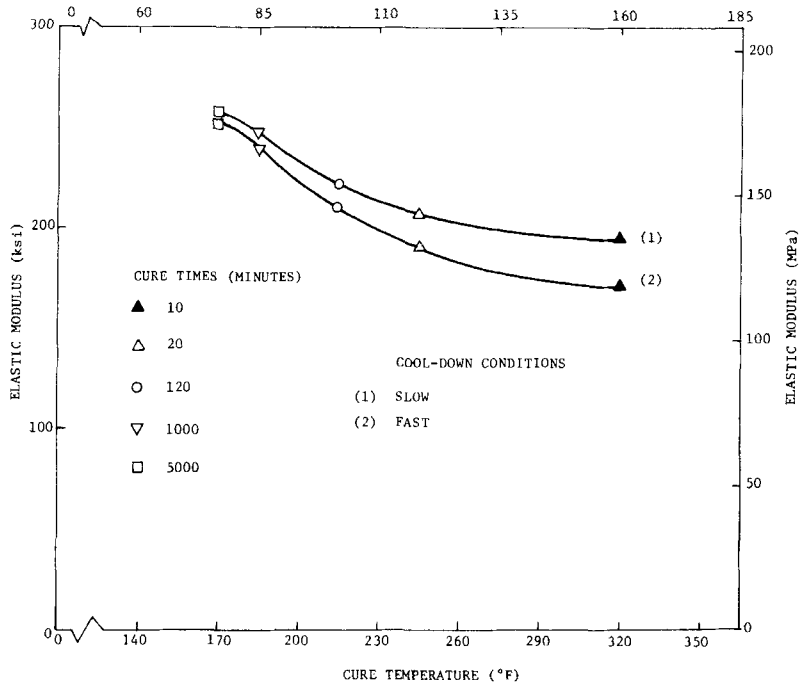

FIGURE 11 Comparison of Metlbond 1113 rigidity-cure optimization curves for the slow and fast cool-down conditions.

provides an alternative method for determination of the fracture stress with the use of the strain energy release rate (G) instead of the use of the stress intensity factor. The expression relating the strain energy release rate (G) to the geometrical parameters and the applied load (P) is given by,[19–21]

$$G = \frac{P^2}{2B}\frac{\partial c}{\partial a} \tag{3}$$

where B is the material thickness in the vicinity of the crack, $\frac{\partial c}{\partial a}$ is the change in compliance (c) and "a" is the crack length. The load level which causes a spontaneous crack propagation is called the critical load, and the corresponding strain energy release rate is called the critical strain energy release rate (G_c).

For a given material the compliance (c) is defined as,

$$c = \delta/P \tag{4}$$

where δ is the displacement. Displacement is a function of the loading mode, consequently the strain energy release rates must be determined according to the mode of loading and hence the mode of failure. There are three principal modes of failures: opening mode with G_{IC}, in-plane shear with G_{IIC}, and torsional shear with G_{IIIC}.

In industrial applications adhesive joint geometries and loading modes frequently produce opening mode failures. Single lap, butt, peel, cone, and cantilever joint geometries produce typical examples of Mode-I failures. In the presence of mixed opening modes, Mode-I usually remains the dominant mode for most engineering applications.

Various theories have been suggested for relating the yield stress (σ_y) and the tensile modulus (E) to the critical strain energy release rate (G_{IC}). For plane-strain, elastic–plastic failure, Kinloch and Shaw[22] suggest the use of

$$G_{IC} \approx 6\pi \frac{\sigma_y^2}{E} r_y (1 - \nu^2) \tag{5}$$

where r_y is the radius of the crack tip deformation zone. Bascom reports[6,15] the magnitude of r_y as $\sim 8 \times 10^{-3}$ in. for a CTBN-epoxy.

The form of Eq. (5) was originally introduced by Griffith.[23,24] He found that crack growth in brittle materials (such as glass) will occur when the rate of change of elastic strain energy $\left(\frac{du}{da}\right)$ is equal to the rate of change of energy required for crack growth $\left(\frac{dW}{da}\right)$. Based on stress field calculations for an elliptical flaw by Inglis,[25] Griffith showed that

$$\frac{du}{da} = G = 2\pi \frac{\sigma^2}{E} a. \tag{6}$$

The rate of change of energy $\left(\frac{dW}{da}\right)$ considered by Griffith was only due to surface energy. On the other hand, for ductile materials, the

$\left(\frac{dW}{da}\right)$ term involves mainly plastic energy due to crack tip plastic deformation. Irwin[26,27] calculated the size (diameter) of this plastic deformation zone (r_p) by considering an infinite plate containing a single crack under the action of tensile in-plane loading perpendicular to the crack. The diameter of the plastic (deformation) zone (r_p) was thus shown to be

$$r_p = \frac{K_{IC}^2}{\pi\sigma_y^2}, \tag{7}$$

where K_{IC} is the critical stress intensity factor for Mode-I loading. Based on Griffith's energy criterion and Eq. (1), the "corrected" critical strain energy release rate could then be written as:

$$G_{IC} = \pi\frac{\sigma_y^2}{E'}r_p. \tag{8}$$

Irwin showed that the plane-strain elastic constraint will increase the tensile stress for plastic yielding and thus affect the size of the plastic-zone. Such an increase in the yield strength (σ_y) was estimated to be by a factor of $\sim\sqrt{3}$.[27,28] The radius of crack tip deformation zone (r_y) can, therefore, be written as:

$$r_p = 2r_y \tag{9}$$

for plane-stress and,

$$r_p = 6r_y \tag{10}$$

for plane-strain conditions. Substitution of Eqs. (2) and (10) in Eq. (8) results in Eq. (5).

Examination of the literature[5,11,13,14,29] reveals that the simplest method for the experimental measurement of G_{IC} is the use of the Tapered Double Cantilever Beam (TDCB) specimen geometry. In TDCB specimens the compliance remains independent of the crack length due to the presence of the "height" taper. O'Connor[5] reports experimental G_{IC} values for Metlbond 1113-2 adhesive in the bonded form, measured with the use of TDCB geometry. It should be noted that the G_{IC} values obtained for an adhesive with the use of bulk and

bonded TDCB specimens are not necessarily the same. Bascom[11] reports that, with bonded TDCB specimens, the maximum value of G_{IC} is obtained when the crack tip deformation zone diameter ($2r_y$) is approximately equal to the bond thickness. Bascom's results also reveal that for a CTBN-epoxy this "maximum" G_{IC} is approximately equal in value to that obtained with the use of a bulk TDCB specimen.[11]

For the present investigation, the critical strain energy release rate values for the extreme cure conditions are calculated with the use of Eq. (5) by assuming $r_y \approx 8 \times 10^{-3}$ in[6,15] (Table I). The reported value[8,9] of Metlbond adhesive Poisson's ratio ($v \approx 0.37$) is used for these calculations. Apparently the optimum value of G_{IC} is achieved with cure at a high temperature and short time and with the adhesive without the carrier cloth. The measured G_{IC} values for Metlbond 1113–2 (as reported by O'Connor[5]) are shown in Table II-A. As mentioned earlier, O'Connor used bonded TDCB specimens to measure the G_{IC} values. Since the bond thicknesses which were used in his investigation (0.025–0.030 in) were larger than the typical r_y values for epoxies (as reported by Bascom,[6,15]) his measured G_{IC} values were assumed to be comparable to our calculated values for the same material. Apparently for 260°F cure, the measured value of $G_{IC} = 41.22$ in-lb/in^2 (for 70 minutes cure) is in close agreement with our calculated value of $G_{IC} = 40.20$ in-lb/in^2 (for 20 minutes cure) when the slow cool-down condition is used (Table II-B). The 50-minute difference in cure times of the compared values is assumed to be insignificant as the calculated 1113-2 G_{IC} values for 5000 minutes cure and 10 minutes cure are different by only 10% (Table I).

Examination of the literature reveals that the calculated values of crack tip deformation radius (r_y) increase with increasing environmental (test) temperature.[13] Our experimental observations regarding increased ductility and plastic flow with high cure temperatures and/or long cure times and brittle material behavior with low cure temperatures and/or short cure times also indicate that the measured r_y values should be larger with higher cure temperatures and/or longer cure times. This observation indicates that the G_{IC} values listed in Table I may be different if the exact values of r_y corresponding to the cure conditions of Table I are known. An investigation is now underway by the authors to measure experimentally the values of G_{IC} and thus to determine experimentally the effects of cure conditions on G_{IC}, with the use of single-edge cracked (bulk) specimens. The authors do not expect the cure dependence of r_y to affect the already determined optimization behavior of G_{IC} (*i.e.* high values obtained with high temperature–short

time cure conditions), as the variation of r_y with the cure conditions has been observed (or calculated[13]) to be similar to that of the G_{IC} values.

TABLE I
Calculated G_{IC} Values
($r_y \approx 8 \times 10^{-3}$ in. assumed)

1113 Cured at 115°F for 5000 Minutes
Fast Cool: $G_{IC} = 28.68$ in-lb/in^2
Slow Cool: $G_{IC} = 30.73$ in-lb/in^2

1113 Cured at 320°F for 10 Minutes
Fast Cool: $G_{IC} = 30.15$ in-lb/in^2
Slow Cool: $G_{IC} = 33.34$ in-lb/in^2

1113-2 Cured at 170°F for 5000 Minutes
Fast Cool: $G_{IC} = 29.90$ in-lb/in^2
Slow Cool: $G_{IC} = 34.36$ in-lb/in^2

1113-2 Cured at 320°F for 10 Minutes
Fast Cool: $G_{IC} = 29.18$ in-lb/in^2
Slow Cool: $G_{IC} = 38.25$ in-lb/in^2

TABLE II

A—Reported G_{IC} Value for 1113-2 in Bonded Form (TDCB Specimens)

260°F, 70 Minutes Cure with Low Pressure and Slow Cool-Down (8 Hours)

Average for 2 in/min Heat Rate Tests

$$G_{IC} = 41.22 \text{ in-lb/in}^2$$

Overall Average from Various Head Rates

$$G_{IC} = 40.64 \text{ in-lb/in}^2$$

B—G_{IC} Value for 1113-2, Calculated with the Use of the Formula:

$$G_{IC} = 6\pi \frac{\sigma_y^2}{E} r_y (1 - \nu^2)$$

260°F, 20 Minutes Cure with Low Pressure and Slow Cool-Down (12 Hours)

$$G_{IC} = 40.2 \text{ in-lb/in}^2$$

CONCLUSIONS

The authors believe that the results of the present investigation permit the following conclusions:

1) It is possible to optimize the ultimate and fracture strengths, rigidity and cost with respect to the cure temperature, time and cool-down conditions.

2) The ultimate strength and rigidity are higher at the cure conditions of low temperature–long time in comparison to the high temperature–short time on the optimization curves for Metlbond 1113 and 1113-2.

3) For the adhesive with the carrier cloth (1113) the slow cool-down condition results in a higher ultimate strength and rigidity optimization behavior in comparison to the fast cool-down condition.

4) For the adhesive without the carrier cloth the slow cool-down condition results in a higher ultimate strength behavior in comparison to the fast cool-down condition.

5) An increase in the cure pressure results in an increase in the adhesive tensile strength.

6) An increase in the cure temperature causes an increased amount of degradation.

7) The G_{IC} values measured using the bonded TDCB specimens and the values calculated with the use of the theoretical formula based on the plane-strain assumption, measured tensile properties and reported crack tip deformation radius value, show good agreement.

8) The optimum G_{IC} value is obtained with the high temperature–short time cure condition, in the absence of carrier cloth.

The authors believe this important result to be the reason for the UHU recommendation[16] of high temperature–short time cure schedules for the bonded specimens. Apparently the single lap specimens bonded with the UHU thermosetting adhesive yield the highest strength when cured with high temperature–short time cure conditions. On the other hand, the authors believe that the strength values measured and reported by the UHU product information brochure represent fracture stresses, rather than adhesive yield stresses. The failure of adhesively bonded joints is often due to catastrophic crack propagations originating from inherent flaws or impurities on the adhesive–adherend interface. Hence, complete characterization of adhesives requires investigation of its fracture energy (and thus fracture stresses) as a function of different cure and service conditions as described in this paper.

Acknowledgements

The material covered in this paper is based upon work supported by the National Science Foundation under Grant No. CME-8007251.

References

1. M. Chmura and E. McAbee, Correlation of mechanical properties of resins obtained

in an adhesive joint and in bulk form, *Technical Report 3330* (Picatinny Arsenal, Dover, NJ, April 1966).
2. J. K. Gillham, A semimicro thermomechanical technique for characterizing polymeric materials: Torsional braid analysis, *J.A.I.CH.E.*, **30**, 1066–1079 (1974).
3. E. Sancaktar and H. F. Brinson, The viscoelastic shear behavior of a structural adhesive, *Virginia Polytechnic Institute Report No. VPI-E-79-33* (September 1979).
4. D. W. Dwight, E. Sancaktar and H. F. Brinson, *Polymer Science and Technology Series*, **12A**, L. H. Lee, Ed. (Plenum Press, N.Y., 1980) pp. 141–164.
5. D. F. O'Connor, Factors affecting the fracture energy for a structural adhesive, Master's Thesis, Virginia Polytechnic Institute and State University, Blacksburg, VA, August 1979.
6. W. D. Bascom, C. O. Timmons and R. L. Jones, *J. Matls Sci.* **10**, 1037–1048 (1975).
7. E. Sancaktar and H. F. Brinson, Adhesion and adsorption of polymers, *Polymer Science and Technology* (Plenum Press, NY, 1980), pp. 279–300. L. H. Lee, Ed.
8. H. F. Brinson, M. P. Renieri and C. T. Merakovich, *Fracture Mechanics of Composites*, ASTM STP 593, (ASTM, Philadelphia, 1975), pp. 177–199.
9. M. Renieri, C. T. Herakovich and H. F. Brinson, Rate and time dependent behavior of structural adhesives, *Virginia Polytechnic Institute Report No. VPI-E-76-7*, April 1976.
10. L. J. Hart-Smith, Air Force Conference on Fibrous Composites in Flight Vehicle Design, Dayton, Ohio, September 1972.
11. W. D. Bascom, R. L. Cottington and C. O. Timmons, *Naval Engineering Journal*, pp. 73–86, August 1976.
12. W. D. Bascom, R. L. Cottington and C. O. Timmons, *J. Appl. Polym. Sci., Applied Polymer Symposia* **32**, 165–188 (1977).
13. W. D. Bascom and R. L. Cottington, *J. Adhesion* **7**, 333–345 (1976).
14. W. D. Bascom *et al.*, *J. Appl. Polym. Sci* **19**, 2545–2562 (1975).
15. W. D. Bascon, R. L. Jones and C. O. Timmons, *Adhesion Science and Technology* **9B**, 501–511 (1975).
16. UHU-PLUS Adhesive Product Information Brochure, UHU Linger and Fischer, 758 Bühl (Baden), West Germany.
17. Metlbond 1113 Adhesive Product Information Brochure, Narmco Materials Division, Whittaker Corp., Costa Mesa, California.
18. G. R. Irwin, *J. Appl. Mechanics* **24**, 361 (1957).
19. R. W. Hertzberg, *Deformation and Fracture Mechanics of Engineering Materials* (John Wiley and Sons, Inc., New York, 1976).
20. D. Brock, *Elementary Engineering Fracture Mechanics* (Noordhoff International Publishing, Leyden, Metherlands, 1974).
21. G. P. Anderson, S. J. Bennet and K. L. Devries, *Analysis and Testing of Adhesive Bonds* (Academic Press, Inc., New York, 1977).
22. A. J. Kinloch and S. J. Shaw, *J. Adhesion* **12**, 59–77 (1981).
23. A. A. Griffith, *Phil. Trans. Roy. Soc. of London* **A221**, 163–197 (1921).
24. A. A. Griffith, *Proc. 1st Int. Congress Appl. Mech.* (1924) pp. 55–63, Bienzo and Burgers ed. Waltman (1925).
25. C. E. Inglis, *Proc. Inst. of Naval Architects* **60**, (1913).
26. G. K. Irwin, "Fracture," *Handbuch der Physik VI* Flügge, Ed. (Springer, 1958), pp. 551–590.
27. G. R. Irwin, *Proc. 7th Sagamore Conf.*, p. IV, **63** (1960).
28. S. T. Rolfe, J. M. Barson, *Fracture and Fatigue Control in Structures, Applications of Fracture Mechanics* (Prentice-Hall, N.Y., 1977).
29. S. Mostovoy, E. J. Ripling and C. F. Bersch, *J. Adhesion* **3**, 125 (1971).

NOMENCLATURE

K	stress intensity factor
G	strain energy release rate
E	elastic modulus
v	Poisson's ratio
p	applied load
c	compliance
a	crack length
δ	displacement
G_{IC}	critical strain energy release rate
σ_y	yield strength
r_y	radius of the crack tip deformation zone
$\frac{\mathrm{d}u}{\mathrm{d}a}$	rate of change of elastic strain energy with crack length
$\frac{\mathrm{d}w}{\mathrm{d}a}$	rate of change of energy required for crack growth
r_p	diameter of the crack tip plastic deformation zone
K_{IC}	Mode-I critical stress intensity factor